15 Uncertainty assessment

A considerable effort has been spent on assessment of previously know and newly discovered uncertainties. Aspects related to the environmental design basis, hydrodynamic effects, analysis and modelling effects and parametric resonance were considered. This chapter summarizes key findings and improvements from the current project phase.

The full list of topics can be found in Appendix G Enclosure 16, ref. [16]. Topics that are not included herein are viscous damping on pontoons, inhomogeneous sea states, simulation parameters (simulated time, time step, ramp-up duration), shear lag effects, extreme value estimation of stresses, characteristic load vs characteristic response, dynamic effects of traffic on the bridge, imperfections and parametric excitation.

15.1 Environmental design basis

15.1.1 Sensitivity of response along the metocean contour lines

Problem description

For the estimation of long-term response with the environmental contour method, the design point should be taken as the point along the contour which gives the most severe response. It has been assumed that it is the point along the contour with the largest value of Hs that gives the most severe response. However, this may not be the case and therefore the validity of this assumption has been investigated.

Performed investigation

The validity of the max Hs assumption is checked by including more sea states on the contour line and comparing the sea states that maximizes the individual responses from this extensive screening (5 points along the contour) with the simplified screening (only the point with max Hs). Five sea states are selected for each contour line; maximum significant wave height, maximum peak period and three sea states in between. This investigation is presented in the memo [17].

Findings and recommendations

The maximum response is not found at the maximum Hs but rather at a somewhat higher period. As the eigenmodes are closely spaced in this area this indicates that a slight increase in the period excites a different eigenmode in which higher response is observed for a lower wave height. However, the error in the response is only a few percent on most cases and around 10 % for the worst cases.

15.1.2 Uncertainties in the metocean contour line approach

Problem description

The ultimate goal of a long-term response analysis is to identify the response value with a given return period. More specifically, we seek the characteristic response value r_q, which has a specified annual exceedance probability q. This is referred to as the q-probability response or the $1/q$-year response.

The q-probability response is most accurately determined by a full long-term approach. However, due to the large computational cost associated with this approach, the environmental contour method is used to obtain reasonable estimates of the q-probability response. Recently, methods have been developed which provide more accurate estimates of the q-probability response at a significantly reduced computational cost [18, 19]. These methods are referred to as inverse reliability methods. The relation between the full long-term approach, the environmental contour method and the inverse reliability methods is explained in detail in a separate memo [17].

Performed investigation

In the Bjørnafjorden project so far, environmental contour lines have been applied to identify which sea states that give rise to the q-probability response. An assessment of the validity of the contour line approach is carried out in [17] for the concept K12_07. The 100-year response due to wind waves was calculated by an inverse reliability method, using joint distributions of Hs and Tp for each directional sector which were provided by the client. The provided (Hs,Tp)-distributions were the same distributions that the environmental contours reported in the metocean design basis are based on. However, the environmental contours that are reported therein have been adjusted in order to give more correct 100-year Hs values. Thus, the environmental model used with the inverse reliability method was not validated for direct use in a long-term response analysis. Still, the model was used to give an indication of the accuracy uncertainty of the contour line approach. The 100-year response due to wind waves was calculated for 20 different responses along the K12_07 concept using an inverse reliability method. The results were compared with the 100-year response estimates from the contour line approach.

Findings and recommendations

Even if the results in the performed investigation are based on an environmental model that is not validated for use in long-term response estimation, they give an indication that the estimates of the long-term response produced by the contour line approach might be too rough in some cases. It is however not possible to draw any definite conclusion without a comparison with a full long-term approach. Further studies on the long-term response are therefore recommended. An environmental model suited for use in long-term response analyses should be established, and full integration of the long-term response formulation should be carried out for some selected cases.

It is also important to be aware that environmental contours corresponding to a given return period are not uniquely defined. Different methods exist to produce them, and these can give quite different results [20, 21, 22], especially when sector dependence is included [23].

15.1.3 Wind spectrum parameters

Problem description

Table 15 in Metocean Design Basis indicate that the measurements on site shows large variation in wind input parameters. The values are tabulated as P10, P50 and P90 values. It is not clear which to choose in design calculations. Including all possible variations of the parameters will lead to an ineffective design procedure.

Performed investigation

Since Table 15 values influence dynamic response due to wind, the effect of varying the following parameters has been studied: xLu, Au, cux and Cuy. The analysis was performed for wind response only and for all wind directions. P50 values were chosen as reference if not specified otherwise.

Findings and recommendations

For variation of xLu the standard deviation of the response follows the reference value within +/- 10%. Low and high xLu values give lowest response. The results indicate that the highest response value for this concept is for an xLu value in medium range.

For variation of Au the standard deviation follows the reference value within +/- 10%. The general trend is that increased Au values gives increased response.

For variation of Cux the standard deviation follows the reference value within +/- 10%. The effect of change of cux is small for wind perpendicular to the alignment and more pronounced as the wind comes along the alignment. The Cux value of 3.0 used in the reference case gives the highest value of the calculated cases and increase of Cux value gives reduced response.

The response is sensitive to changes of the Cuy parameter, particularly for wind perpendicular to the alignment. Lower value of Cuy gives higher response, and Cuy values below the P10 value of 6.4 will increase the standard deviation of the response with more than 20%. For skew wind, where the wind is more along the alignment, the effect is less pronounced.

The findings are not universally valid, as it will be dependent on eigenfrequencies of the structure compared to the spectral distribution of wind. In order to be able to do an effective design we recommend that:

- Wind data is studied to see if the spread of the P10-P90 values can be reduced
- Further analysis is performed on the selected concept to conclude on which parameters to use in design.

15.2 Hydrodynamics

15.2.1 Wave-current interaction

Problem description

When a current is present together with waves, the wave loads (both radiation and diffraction loads) are modified due to wave-current interaction effects. This modification consists in 1) a pure Doppler frequency shift because the wave encounter frequency depends on the current and 2) additional terms in the hydrodynamic problem to be solved that depends on both the velocity potential and the current speed.

Performed investigation

The wave-current interaction effects are investigated by performing numerical analysis with a single pontoon in Wasim, considering different combinations of wave and current directions as well as current speeds. The results are compared to Wadam results (where the effect of current is not considered in the hydrodynamic problem) with the encounter period modified due to a pure Doppler shift. This comparison was done to 1) validate the Wasim results for zero current speed and 2) to investigate the importance of wave-current interaction effects beyond this frequency shift.

The hydrodynamic transfer functions for wave excitation loads as well as radiation loads (added mass and damping) from the Wasim analysis were imported into the global OrcaFlex model in order to investigate the effect on global responses.

Findings and recommendations

The comparison between Wasim and Wadam analyses showed that wave-current interactions may have a significant effect on wave excitation loads beyond a pure frequency (Doppler) shift. The effect was more significant for sway and roll than for heave. The effect on added mass and damping was much less pronounced. Importing the Wasim transfer functions into OrcaFlex revealed an increase in global responses such as the strong axis moment. The effect of wave-current interactions is more severe for K13 than for K12. The analysis is however done only with a current speed of 1.5 m/s, assumed uniform over the span of the bridge, and with current either aligned with or opposite of the wave direction. In order to have a better understanding of the significance of wave-current interaction effects, more detailed metocean data is required. Information about the instantaneous spatial variation of current across the fjord as well as the joint distribution of wave and current directions is needed. It is also a matter of fact that the global response of the bridge is sensitive to wave-current interaction effects, largely because different modes can be triggered depending on the encounter frequency.

Since wave-current interactions have an important effect that should be accounted for in the design, it is recommended to do a further effort to reduce the uncertainty in future phases of the project. This effort should consist in 1) obtaining more accurate metocean data with respect to the joint distribution of waves and current, 2) to validate and verify the numerical model through model tests for a single pontoon and 3) to do more extensive studies on the global bridge model in OrcaFlex. The present assessment of wave-current interaction effects in OrcaFlex is done solely in frequency domain. This assumption should be verified by doing additional studies in time domain. An additional difficulty in OrcaFlex is that the wave spectrum must be modified manually in order to shift its different frequency components. This operation is not straightforward in short-crested waves, and hence only long-crested waves are considered here. Future work should investigate how to properly scale wave spectra for short-crested sea states and further assess the importance of wave-current interaction effects in short-crested versus long-crested waves.

15.2.2 Hydrodynamic interaction

Problem description

Structures in proximity to each other experience hydrodynamic interaction effects in their radiation loads (added mass and damping) as well as in wave excitation loads. One consequence is that the motion of one body introduces radiation loads on other bodies. If the number of structures in the hydrodynamic analysis is N_b, the dimension of the added mass and radiation-damping matrices become $(6N_b \times 6N_b)$. This has consequences for the computational efficiency. If all bridge pontoons were to be considered simultaneously, the CPU time would be excessive and the problem, if studied in time domain, likely prone to numerical instabilities.

Performed investigation

A study has been performed to determine the number of pontoons that are necessary to include in the multibody hydrodynamic analysis. The interaction between adjacent pontoons are related to resonant wave motion, or sloshing, that depends on the distance between adjacent pontoons both with respect to resonance periods and resonance-induced amplification. To assess the effect on global responses, the hydrodynamic coefficients from multibody analysis with span widths 100 m and 125 m, respectively, were imported into OrcaFlex for frequency domain analysis.

Findings and recommendations

The hydrodynamic analysis demonstrated that it is generally sufficient to consider three pontoons in a multibody analysis, i.e. to determine the loads on a pontoon it is enough to consider on adjacent pontoon on each side. Only small changes were observed by increasing the number of pontoons in the analysis to five or beyond. From the frequency domain OrcaFlex analysis, hydrodynamic interaction effects appear to either have little effect on or reduce the maximum bending moments about the strong axis. The bending moment about the weak axis is found to be more sensitive, especially with 100 m span width. The analysis indicates that hydrodynamic interaction effects may be more important in fatigue sea states than in ULS conditions.

The method used to study global responses in frequency domain is incomplete in the sense that some coupling terms are neglected. Future studies should consider global time domain analysis. This was also attempted here but failed due to instabilities/convergence issues related to the so-called retardation functions (the time domain equivalents of the frequency domain added mass and damping). More effort is required to overcome this issue. One possibility that was not addressed in [11] is to neglect certain terms that are not considered important for the physical response, but that nevertheless can generate numerical problems. This has indeed been the experience when working with side-by-side mooring of LNG vessels, where the gap between the bodies is smaller and the hydrodynamic interaction stronger. Another measure that may improve the retardation functions is to use a lid in the hydrodynamic analysis in Wamit, where artificial damping is added to the free surface in order to avoid unrealistic sloshing wave elevations. This is also known to have a beneficial effect on the convergence and stability of the time domain retardation functions. The damping associated with such lids is however in general sea state dependent, and a careful calibration against model tests is necessary in order to obtain realistic values. This should be considered as future work, i.e. performing model tests designed to investigate hydrodynamic interaction effects and to calibrate the lid damping coefficient in the Wamit analysis. Such model tests need to be carefully planned in order to be valuable. The calibrated time domain model will indicate whether the frequency-domain approach is appropriate. With a validated model, it is recommended to do further analysis to investigate the influence of hydrodynamic interaction effects on fatigue life for the chosen concept.

15.2.3 Second order effects

Problem description

Second-order effects may give rise to mean, difference-frequency and sum-frequency wave loads. The difference-frequency loads and sum-frequency loads give rise to low- and high-frequency loading, respectively, that may be important if they coincide with important resonance periods. The classical example involving difference-frequency excitation is resonant slowly-varying wave drift loads on a moored structure with high natural periods in surge, sway and yaw. A typical example of sum-frequency excitation is resonant heave motions of a TLP with natural heave period in the range 2-4 s. In order to compute these second order loads, a second order hydrodynamic analysis must be performed. This is much more time consuming and sensitive to mesh refinement than a "standard" first order analysis, and requires that the free surface is discretized in order to satisfy second order free-surface conditions. Slowly-varying loads are often approximated from the mean wave drift loads by using the Newman approximation. The mean wave drift loads can be obtained from a first order hydrodynamic analysis. The Newman approximation is therefore a popular and widely used simplifying assumption. In general, the Newman approximation is valid when the relevant natural periods are in the order of 100 s or more and when the water depth is not very shallow. Such approximate methods are not available or well-established for sum-frequency loads.

Performed investigation

A second-order hydrodynamic analysis in Wamit was performed to calculate transfer functions for difference-frequency loads (so-called full QTF) for a single pontoon without any current.

Findings and recommendations

The analysis performed in the present phase of the project indicated that Newman's approximation is sufficiently accurate to predict the slowly varying horizontal-plane excitation of the pontoons. There are however issues to be further clarified, such as the slowly-varying drift loads and damping of slowly-varying motions due to wave-current interaction effects. For the present project, the current is more significant relative to the water particle velocities than in traditional offshore applications, and it is not evident that traditional methods are valid. In order to study this in more detail, a combination of dedicated model tests and advanced numerical methods (either non-linear potential flow or CFD methods) are recommended. It should also be investigated if there are important viscous contributions to the slowly-varying wave loads, especially when the current speed is significant.

Sum-frequency loads have not been addressed in the present phase of the project. However, because the global bridge response has natural periods over a large period band from very small to large periods, one cannot conclude that these loads are not important. For instance, in a sea state with peak period $T_p = 6\ s$, there will be energetic wave components with e.g. periods $T = 5\ s$ and $T = 7\ s$ giving rise to sum-frequency loads with frequency $f = \frac{1}{7\ s} + \frac{1}{5\ s} = 0.343\ hz$, i.e. a period of approximately 2.9 s. It is possible that such difference-frequency loading, particularly in heave, roll and pitch, may induce global responses in the bridge, especially considering that the piston mode on the pontoons is in this period range (e.g., the mode in which every other pontoon goes up or down causing large weak-axis moments). It is therefore recommended to do a numerical study also of second-order sum-frequency effects in future phases of the project. In planning such study, one must be aware that sum-frequency effects can pose a numerical challenge with respect to convergence and stability. A thorough assessment of the numerical convergence is thus appropriate.

15.2.4 Freeboard exceedance

Problem description

If water exceeds the freeboard of one or several pontoons, loads that influence the global response of the bridge may occur. The pontoon freeboard is set to 3.5 m, so that the incident wave elevation or the pontoon motions alone are not enough to induce negative freeboard. However, one must consider the possibility that the combination of large sea states, pontoon motions, wave-current interaction effects and non-linear diffraction effects may lead to water exceeding the freeboard.

Performed investigation

Several alternatives were considered to model the effect of freeboard exceedance. One of these was to simply reduce the heave, roll and pitch restoring coefficients of the pontoon. This alternative was however considered inadequate, since 1) the restoring is related to the linear motion of the floater and not the relative wave elevation and 2) it does not reflect the fact that freeboard exceedance is a transient phenomenon and so also the imposed loads will be of transient nature. Instead, a simplified wave-on-deck model was adopted, where shallow-water flow is assumed on top of the pontoon. The pontoon was divided into several strips, and the relative wave elevation above the pontoon's deck level was extracted in the centre of each strip. In doing so, the incident wave elevation was multiplied with an amplification factor to account for wave non-linearity and local diffraction effects. If at a given time step the relative wave elevation is so that the wave exceeds the freeboard, a vertical force is computed for the strip; otherwise, the vertical force is zero. The vertical forces on all strips are accumulated to a vertical force and a roll moment that are imposed as external loads in the pontoon's equations of motion. Hence, the model, although simplified, is physics based and can reflect the transient type of loading. The wave amplification factors are deliberately chosen somewhat on the conservative side. To investigate the effects of freeboard exceedance on the global bridge response, studies on a single pontoon were first conducted in a 100-year and 10000-year sea state with and without wave spreading, respectively. The model was also implemented in a global OrcaFlex analysis for a 100-year sea state and an exaggerated 10000 year sea state, respectively.

Findings and recommendations

For the single-pontoon model, freeboard-exceedance events were observed in the 100-year sea state with moderate influence on the heave and roll motions. In general, freeboard exceedance may lead to both reduced motion (damping) and amplified motion (excitation). This is largely governed by the length of the force impulse divided by the relevant natural period. In the 10000-year sea state, significant amplification of the heave motions was observed, while the roll motion was unaffected or slightly reduced. When incorporated in the global model, freeboard exceedance was found to have negligible influence on strong and weak axis bending moments in the 100-year sea state while leading to a slight increase in the exaggerated 10000-year sea state. The analyses performed with the proposed model here indicates that 1) freeboard exceedance may occur in 100- and 10000-year sea states, but 2) has un-dramatic consequences for the global bridge response. In addition, a larger number of sea states should be considered. The proposed freeboard model should be validated and possibly calibrated against CFD analysis and/or dedicated model tests. CFD analysis or model test should also be used to investigate the relationship between wave-current interaction effects and freeboard exceedance. If the model proposed in the present phase is found to be inaccurate, there are more refined models available where the flow on deck of the pontoon is resolved in space and time through solving the shallow water equations.

15.3 Analysis, modelling and response

15.3.1 Mooring line damping

Problem description

The mooring lines contribute significantly to the global damping for many of the deformation modes of the bridge. This large effect was not properly documented in Phase 3 of the project and raised as an uncertainty at the beginning of Phase 5.

Performed investigation

Several types of investigations were performed in the work to better understand the global effect of mooring line response:

The methodology and input coefficients used for mooring line damping was checked, and found to be aligned with conventional offshore practise.

A preliminary sensitivity study was conducted in which the effect of pretension, drag coefficients etc. was investigated on a mooring cluster, ref. [24]

An analytical approach to mooring line damping based a quasi-static considerations was developed, in which a nonlinear mooring cluster damping characteristic was extracted, ref. [25]. The findings compare well with findings from the offshore industry. The local dynamic line response is small compared to the quasi-static contribution from lateral motion of the pontoon.

Decay testing was performed on the global model in Orcaflex in which the mooring lines were included with the relevant viscous drag coefficients. The bridge was deformed into mode shapes based on an eigenmode analysis and released, and the corresponding modal damping level was found. Results with and without mooring were compared, and the moorings were found to be a significant source of modal damping for the modes in which significant pontoon motions was present. See Appendix F [4] for more details.

The effect of global bridge deformations due to transverse loads, temperature and tide affects the mooring line pretension, but the effect on global modal damping is limited and within acceptable limits.

Findings and recommendations

With the performed investigations the uncertainty with the global effect of mooring line damping is removed. The physics behind the damping is now documented and found in agreement with published results from the offshore industry.

15.3.2 Spectrum discretization

Problem description

The wave spectrum is discretized into a set of discrete wave components which are simulated in time domain. Whether a structural eigenmode is excited or not depends on the frequencies of the wave components present in the simulation. The magnitude of the structural response depends on the wave energy (amplitude) present in the wave components. It is therefore important to discretize the wave spectrum into enough wave components close to the important structural eigenmodes to avoid unrealistic responses. To keep the calculation time to a minimum the total number of wave components should be kept to a minimum.

Performed investigation

In OrcaFlex, the wave spectrum may be discretized using three different approaches:

- Arithmetic progression (constant frequency increments with varying wave amplitude)
- Geometric progression (constant ratio between successive frequencies with varying wave amplitude)
- Equal energy (constant wave amplitude with varying frequency increments)

Arithmetic progression requires a high number of wave components to avoid signal repetition and should therefore not be used to discretize a wave spectrum in OrcaFlex as the calculation time will increase drastically.

The wave discretization was studied by applying the equal energy approach with 150 to 750 wave components in 10 seeds of 3600 s. In the equal energy approach, the frequency increments between wave components are inversely proportional to the wave spectrum energy. If little wave energy is present near important structural modes, the response may therefore be unrealistic due to few wave components. To refine the discretization near these frequencies the total number of wave components may have to be increased quite a lot.

A refined discretization method was also developed to improve the shortcomings of the equal energy approach. In this method, a frequency increment distribution is used to ensure enough wave components where they are needed.

Findings and recommendations

It was found that approximately 600 components were enough to achieve convergence for the important forces and moments. It is thus confirmed that the wave spectrum discretization used in the global analysis are converged.

Using the refined discretization method, the number of wave components may be reduced to about 150 components without compromising the precision of the results. The calculation time could therefore be decreased substantially by applying the refined discretization method.

15.3.3 Shear stiffness

Problem description

The beam element in Orcaflex does not account for shear stiffness, which may be relevant for certain weak-axis modes. Simplified investigations were performed in the previous phases of the project to assess the effect, and it was found to be of minor importance, but the uncertainty was not closed.

The effective shear areas of the bridge girder in the vertical direction are low, and accounting for shear deformation may as such reduce the stiffness of the girder which again increase the modal periods. Shear deformation may also be relevant in the strong axis in which the width of the cross-section is 4-5 times the span length of the girder between pontoons. However, environmental loads will not trigger the strong-axis deformation to a notable extent.

Performed investigation

Simulations with and without shear stiffness were conducted in RM-bridge in which this can be selected as an option in the element formulation, see [26] for details. Two types of simulations were conducted; eigen mode calculation and a time-domain response assessment with wind loading.

The eigenmode calculations show a shift in the period of the vertical piston modes (every other pontoon up or down) of around 5%, whereas quasi-static assessment of the same mode yields a change of around 8 %. The modal period is between 2-3 seconds, in which there is significant wave loading for all modes. Hence, the shift in eigen period due to shear stiffness will not affect if the piston mode is excited in wind sea conditions (e.g., the mode in which every other pontoon goes up or down causing large weak-axis moments).

The wind response assessment revealed a shift in the response around 3 seconds (as for the eigen period) and around 1 seconds. The latter is a vibrational mode of the bridge girder that is not excited by environmental loads to an extent at which it is governing for design.

Findings and recommendations

The investigation revealed a 5-10% difference in weak-axis piston eigen mode, and some change in the lower period vibrational modes internally in the bridge girder. This does not lead to a significant change in response, and the lack of shear stiffness in Orcaflex is as such considered not to be a concern for the global response of the bridge.

15.3.4 Coupled vs. uncoupled response

Problem description

The main design method in previous phases has assumed uncoupled environmental conditions (such as wind sea, swell and wind), and verified this with a limited amount of simulations with coupled environmental conditions. For linear processes with linear response decoupling is a valid assumption. However, mooring line response is nonlinear so that e.g. temperature and tide change the linear stiffness of the system due to the change in static pontoon position.

The response of the bridge is a complex process, and the "true" response is coupled. However, this requires accurate input data with fully correlated data for all environmental contributions and a vast amount of simulations in order to be the only design method.

Performed investigation

It was decided to maintain the uncoupled approach as the main design method, but the checks with the coupled approach was more elaborate than in previous phases. The same environmental conditions were investigated using a coupled and decoupled approach. The effect of temperature and tide was checked with separate coupled simulations. Ten seeds were used for each condition, and the AUR method was used to estimate the 90-percentile response. This was compared to the expected maximum found using the decoupled approach.

For axial force, the coupled approach was found to yield somewhat higher response. However, weak- and strong-axis bending moment was reduced in the coupled simulations. Especially swell caused large differences, in which the decoupled approach gave a pure excitation of a mode that was not seen when coupled with wind and wind sea. This is likely due to a combination of aerodynamic damping and disturbance from the wind sea that is not captured for the decoupled approach.

The resulting stresses were for all points considered worse for the decoupled approach, and the design of the bridge was thus based on a safe set of response data.

Findings and recommendations

With the performed investigation, the decoupled approach was found to yield conservative results for design of the bridge girder. Mooring lines were designed according to the coupled approach.

The assumption of decoupled response was thus confirmed as a reasonable design choice that significantly improves the complexity and amount of simulations needed to include the relevant effects in a rational manner.

15.3.5 Comfort evaluation

Problem description

During phase 3 of the project the accelerations of the bridge girder were considered as high, and it was not sure if the root-mean-square acceleration criterion that was used gave meaningful limits of bridge comfort. A more detailed investigation was required during phase 5, and a new overall vibration total value (OVTV) criterion was proposed in the design basis.

Performed investigation

A dynamic model of a vehicle was established based on input from NPRA. The dynamic behavior of the bridge girder due to environmental loads was investigated in detail for all the bridge concepts, and combined with the quasi-static deflection due to the weight of passing traffic.

The dynamic vehicle model was used to assess the vehicle response for both bridge motion and the local motion of the vehicle when subject to local wind loads. The calculated accelerations in the driver's seat in the vehicle model was used as a basis to evaluate the OVTV model.

The findings indicate that the bridge girder motion utilized about 1/3 of the OVTV criterion. However, local wind on the vehicle overutilized the criterion with a factor of 3. The bridge was thus assessed as *fairly uncomfortable* rather than the required *not uncomfortable*. No large differences were observed between the concepts.

Findings and recommendations

Using the OVTV criterion as a basis to perform design development based on the driving comfort is likely an immature approach, and NPRA currently has an academic study underway to define a suitable criterion. Based on the findings during this phase of the project the bridge motion was not a large contributor to the discomfort. Hence, it is deemed fairly uncomfortable to drive in a 1-year storm with the turbulence intensities at the bridge location irrespective of the bridge motion.

It is noted that the wave conditions given in the metocean design basis for phase 5 of the project is considerably less than those given for phase 3, resulting in nearly a 50% reduction in dynamic bridge motion. However, it is not possible to conclude that the absolute level of comfort when using the bridge is at an acceptable level based on the proposed bridge concept and the phase 5 wave conditions. Further work on this is recommended, and a better acceptance criterion for driving comfort would be much appreciated.

15.3.6 Fatigue assessment

Problem description

A full assessment of the fatigue capacity of the bridge is challenging due to the extent of the structure, the complexity of the dynamic behavior and the behavior of local details subjected to both local and global loads. Hence, the fatigue estimate from previous phases had a large uncertainty.

Performed investigation

Several improvements in the methodology have been achieved during Phase 5 of the project:

- The local and global deformation of the bridge is now accounted for for traffic loads, combining the global influence lines with the local tire pressure history to create a local stress-time event in each considered detail.
- A stochastic traffic pattern is defined with traffic in both directions in all lanes, capturing the global and local effect of overtaking vehicles and oncoming traffic.
- Uncoupled and coupled simulation of environmental loads were compared and small differences were found.

The new approach has led to reinforcements of the bridge girder, primarily the top deck plate thickness and the trapezoidal stiffeners in the slow traffic lanes. Further, requirements are developed for placements of longitudinal and transverse welds in plates and stiffeners.

Findings and recommendations

The new approach has considerably reduced the uncertainty related to the methodology of the fatigue assessment for flexible floating bridges.

Some uncertainties remain:

- Coupled global and local response of e.g. the interface between bridge girder and column
- Some local structural optimization is required to achieve sufficient fatigue life
- A traffic load model should be developed based on actual traffic data at the bridge location (a FLM5 model)
- Wave interaction effects and inhomogeneous sea states may affect the fatigue capacity.

15.3.7 Ship collisions

Problem description

Bridge crossings are inherently exposed to collision risk, and the Bjørnafjorden bridge both has significant traffic along the bridge due to its proximity to a major shipping lane and some traffic crossing the bridge due to activities inside of the bridge location. There is significant uncertainty in the estimation of relevant design scenarios to consider, but this is outside of the scope of the AMC group during the project phase.

Further uncertainty is found in the local and global response to a ship impact event; locally how the structures interact and how large forces over how long time that are transmitted to the bridge system, and globally how the bridge responds to such loads and where energy is dissipated.

Performed investigation

The local ship collision response was studies decoupled from the global response, and the assumptions behind this is not strictly valid for the collision durations that were simulated. However, the local methodology itself is of high accuracy, using the best available and most thoroughly verified methodology. The main uncertainty is thus on the selected scenario; impacting vessel type, size, velocity and impact location. Several variations were simulated to mitigate this uncertainty, and the ones considered most unfavorable was used for local and global capacity evaluations.

Significant improvements were achieved on the global collision methodology as opposed to the previous project phases; the local energy dissipation in the collision was not accounted for and the total energy balance was maintained to a much higher level. A wide range of scenarios were simulated to cover possible scenario variations. The global response evaluations as such have a considerable reduction in uncertainty.

Ship collisions were found to be dimensioning for parts of the high bridge and the northern abutment, several of the anchors as well as for the columns connecting the pontoons to the bridge girder. A large uncertainty in the latter is the range of impact angles and associated impact energies that are realistically possible to achieve. Coupled local and global deformation was considered in order to properly study the response. With worst-case assumptions it is possible (but somewhat costly) to get a reasonable design of the columns.

Findings and recommendations

Overall the bridge was found robust to ship collision events. The ship collision scenarios are expected to be reduced considerably in the next project phase due to a re-routing of the navigational channel for ships passing along the bridge, further improving the robustness against ship collisions.

It is recommended to continue the study of ship collision response of the bridge during the next project phase, with emphasis on the response of the columns locally and the high bridge and northern abutment globally. The plastic capacity of the bridge girder should be assessed, and its behavior included in the global model to possible consequences. Coupled simulations with local and global response should be extended to include more structural components and scenarios.

15.3.8 Effect of skew wind

Problem description

Conventionally, wind loading to bridges has been applied based on a decomposition of the wind field velocities in the direction transverse to and along the bridge girder, for which transverse wind generate drag, lift and overturning moments whereas longitudinal wind generate frictional loading. This method was adopted for global simulations herein (neglecting the frictional component)

The alternative approach is to calculate the drag, lift and moments directly in the wind direction, thereby evaluating the actual cross-section of the bridge as seen by the wind with its instantaneous wind coefficients. The angle in the horizontal plane between the wind direction and the bridge transverse axis is herein termed *yaw* angle.

For straight bridges the wind load response will normally be highest for winds transverse to the bridge, and decomposition of the wind field is thus a reasonable approach. For large bridges with curvature in the horizontal plane (such as the preferred K12 concept over Bjørnafjorden) it is more difficult to select a governing wind direction due to the possible effect of skew wind.

Performed investigation

A screening study was performed with varying wind direction based on the conventional approach with wind decomposition in the bridge axis. Winds coming transverse to the line between the Northern and Southern abutment was found to yield highest responses in the bridge girder and selected for design.

The wind load model used in Orcaflex was modified to include the possibility of skew wind by interpolating on a set of wind load coefficients based on the *skew* angle (the method considers all six degrees of freedom between the instantaneous wind direction and instantaneous bridge position and orientation).

A simplified 2D CFD study was conducted to obtain aerodynamic coefficients with varying wind direction relative to the bridge girder. The 2D approach has limitations for larger skew angles, and a full 3D CFD and/or model tests are recommended for future verification.

Based on the skew wind load model a screening of bridge response to various wind directions was performed and compared to the same screening with wind decomposition. The strong-axis moment was highest for wind transverse to the main bridge axis both with and without the skew wind effect. However, with increasing skew angles the bending moment was reduced when not considering skew effects but maintains a similar amplitude if the effect is included. The axial load increased significantly with increasing skew angle when considering the skew effect.

Findings and recommendations

The assessment of skew wind is at a low maturity stage and should be better understood before drawing any conclusions as to the response of the bridge. The aerodynamic coefficients should be evaluated in 3D CFD and compared with model tests. The skew wind effect should be assessed with varying length and radius of curvature of the bridge span to understand when and if the skew effect is important.

It is recommended to continue this study towards the detailed design of the project.

16 Construction and marine operations

The construction and marine operations for the Bjørnafjorden bridge are described by the following processes are presented in this section within:

- Fabrication of the bridge girders
- Construction of the cable stayed bridge and the north abutment
- Assembly of the bridge girder and pontoons with columns into floating bridge sections
- Towing of the bridge sections to site
- Installation of the mooring system
- Installation of the floating bridge sections and final connection in Bjørnafjorden

An overall schedule for the construction of the Bjørnafjorden bridge is presented in the figure below.

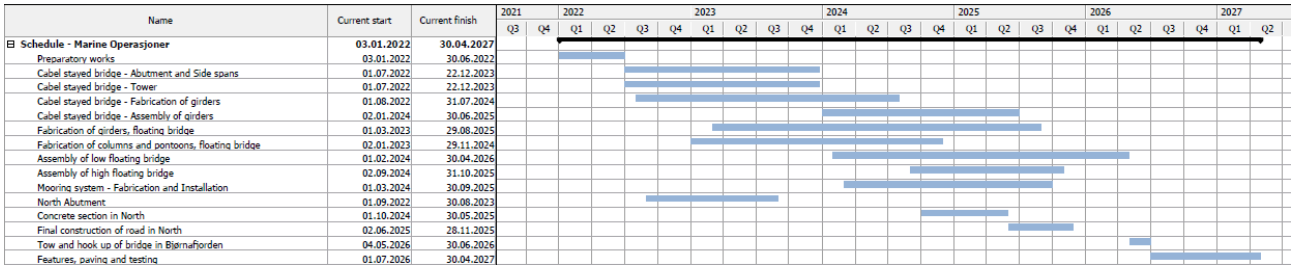

Figure 16-1 Overall schedule for the construction of the Bjørnafjorden bridge

The marine operations are planned according to the DNVGL marine operations standard (DNVGL-OS-H101, H102 and relevant DNVGL-RP-H documents).

The below sections describe a short summary of each phase of the fabrication and marine operations. For further details, see appendix N.

16.1 Fabrication

The fabrication of the bridge girders (25m sections) and pontoons and columns will be performed at fabrication yards typically outside Norway. All elements will be transported to one or more assembly site(s) in the proximity of Bjørnafjorden.

The focus with regards to fabrication has been on the bridge girders suitability for simple fabrication.

Pre-fabrication generally comprises fabrication of stiffeners and panels (i.e. welding on longitudinal stiffeners on to skin plates). Typical stiffeners are shown in Figure 16-2. Trapezoidal stiffeners (U-ribs) are fabricated from steel plates and bent to the specified shape. The ends of the deck U-ribs must be bevelled. The bulb-profiles need no further yard preparations. The spacing between deck U-ribs and bulb profiles is typically 600 mm, whereas for remaining U-ribs 750 mm spacing is used.

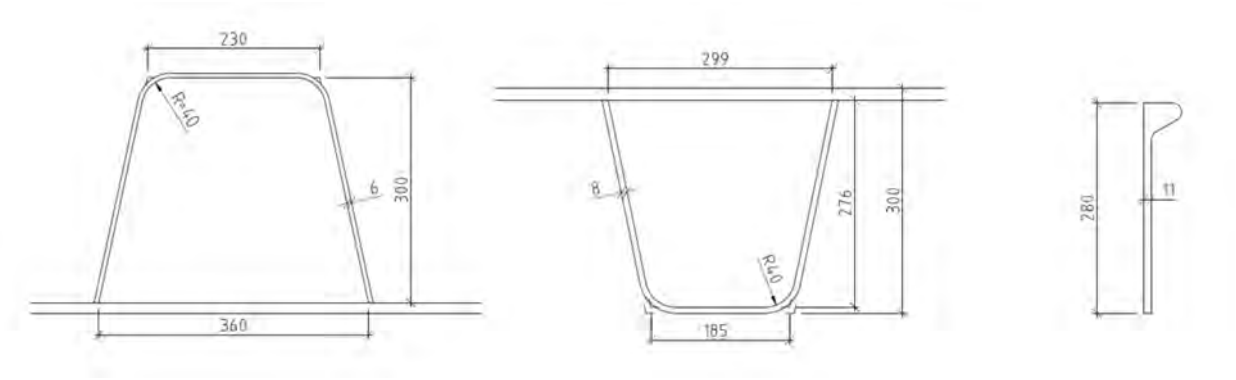

Figure 16-2 Typical stiffener types in longitudinal direction

The longitudinal skin plates for the general section are subdivided into

- 1 deck plate (16 mm)
- 2 vertical plates (12 mm)
- 2 inclined (lower) plates (12 mm)
- 1 bottom plate (12 mm)

For other sections near columns skin plate thicknesses are increased.

The bridge cross-section needs to be subdivided into manageable sizes for panel production and subsequent assembly. In the longitudinal direction a production length of 12.0m is common. It also complies with the need for this length to be multiple of the transverse truss spacing of 4.0 m

In transverse direction, widths will typically be in the range 2.5 m to 3.5 m. This is governed by available sizes from the mill but also handling during fabrication and assembly. This would lead to approx. 18 off such plates per section. The location of panel joints is generally up to the fabricator to choose. The exception to this rule is in the deck structure where direct contact with wheel loads from traffic should be avoided. An acceptable choice is shown in Figure 16-3 ensuring the longitudinal weld seam is close to the centre of the traffic lanes. A width of 3.6 m also ensures joints being in the centre between two adjacent trapezoidal stiffeners (denoted U-ribs in the following). The outlined method adopts an approach where each panel is pre-fabricated with both U-ribs and transverse truss chords necessitates using small width panels.

By this approach, the transverse chords T-beams are also fabricated before panel assembly takes place. This involves cutting webs and flanges in lengths corresponding to the plate widths and making web cut-outs for longitudinal U-ribs and bulbs. The gusset plates for truss diagonals and verticals are also cut and welded on to the flanges (alternatively, for easier intermediate storage by stacking of panels, these items may be welded on just prior to assembly).

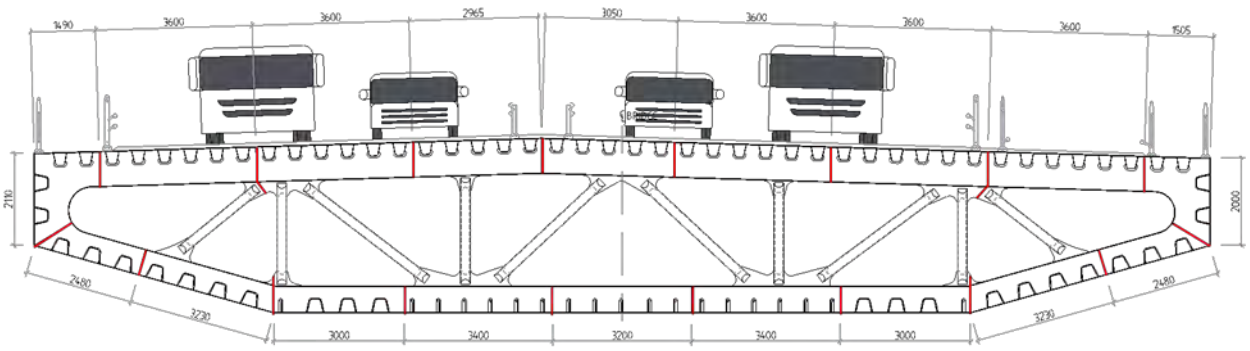

Figure 16-3 Sectioning in transverse direction

16.2 Robot welding of steel bridge elements

16.2.1 Introduction

Welding fabrication of bridge girder elements is typically characterised by:

- Semi-automated welding of plate-to-plate for deck, side and bottom panels as well as bulkheads
- Automated/semi-automated welding of flanges and stiffeners
- All the rest of mainly shorter welds within small compartments make the welds difficult to access using normal welding machines. At present they are therefore generally manual welded. These include welding of bulkheads and T-profiles against panel plates and other welds characterized by varying positions and short lengths.

The above description characterises the present situation within manufacturing of steel bridge elements. Many short welds in varying positions and difficult to access.

This section will focus on the bridge fabrication presently being welded manually. The recent advances within the automation of welding processes will be presented and examples will be drawn to attention where robot automation will have a potential to take over the manual welding.

16.2.2 Advances within automation of the welding process

Advances within automation of the welding process have during the later years been facilitated by:

- much more advanced welding power sources and thus better control of the process
- faster data processing
- adaptive intelligence based on neural networks – the robot will learn and adjust welding parameters during welding
- cheaper robots
- more efficient seam tracking systems, enabling compensation for variations/tolerances
- smaller and lighter robots easy to move around
- robot capable identifying the structure itself and welds automatically

The potential of state-of-the-art welding power sources, robots and computer power may be illustrated by the technologically rather spectacular MX3D bridge project, where state-of-the-art

weld arc control and robot programming technology are demonstrated, resulting in a footbridge entirely made of weld metal, see Figure 16-4.

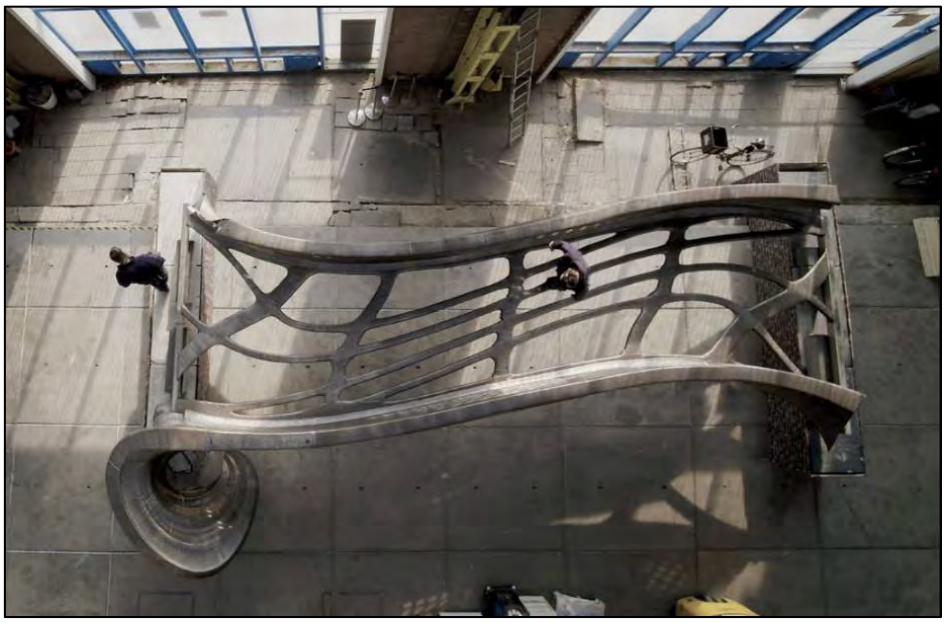

Figure 16-4 Bridge entirely made of weld metal (3-D printed) by means of robotic welding. MX3D project, Amsterdam

16.2.3 Welding automation suitable for large steel structures

In Denmark, extensive research and development (R&D) efforts have been put into robotization of the welding of large steel structures, with major development being achieved at the OSS Lindø shipyard until it closed down. Figure 16-5 shows a large welding robot station for fabrication of sub-assemblies at OSS Lindø.

Figure 16-5 Large robotic welding station at OSS Lindø shipyard

Figure 16-6 shows the results from a cooperation project between OSS Lindø, Migatronic and FORCE Technology - a self propelled welding tractor travelling on magnetic wheels with a grip force of 0.5 tons. The tractor would follow the wobbling and yawing path of the weld groove, and artificial intelligence based on neural networks would adjust welding parameters as well as weaving pattern, as a function of variations in welding groove geometry – especially varying gap.

Figure 16-6 Self propelled and self positioning welding tractor for fully automated welding of section joints in the dock of OSS Lindø shipyard, using adaptive control to compensate for variations in groove position and gap

A spin-off from OSS Lindø shipyard is now a "Robotic Valley" around Odense on the island of Fyn, with several very successful new companies, the most famous being Universal Robots.

A relevant robot supplier for the present applications could however be a company like Inrotech, another robot tech company near Odense with speciality of manufacturing moveable robots mounted on a modular light weight rail system. The robot identifies the structure itself and welds automatically. The company spawned from extensive R&D activities at OSS Lindø within welding in confined spaces, where duty cycles are especially low, entailing high costs for manual welding.

The application can be seen on https://www.youtube.com/watch?v=Xe2LKEJxtdM.

Figure 16-7 shows a later moveable robot solution by Inrotech, robotic welding between webs, stiffeners and deck plate. The robot identifies the structure by itself, and welds automatically. In this case, the robot travels on a modular, lightweight rail system which can be repositioned and extended as needed.

A demonstration of identification of geometry and subsequent welding can be seen on https://www.youtube.com/watch?v=LTU7MTEqX1E.

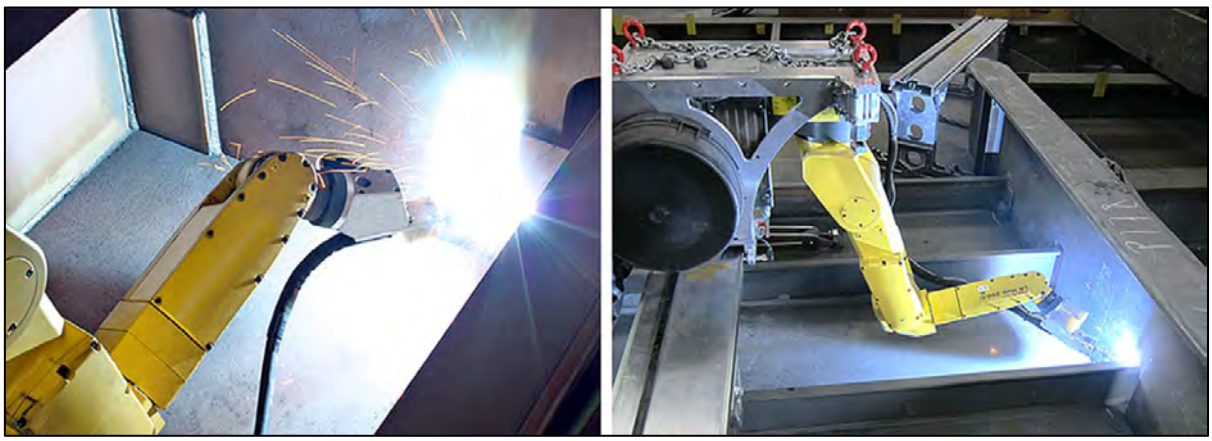

Figure 16-7 Robotic welding between webs, stiffeners and deck plate. The robot identifies the structure itself and welds automatically

A relevant steel manufacturer within Norway, could be a company like Kleven, located at Ulsteinsvik outside Ålesund. The company has utilised automat and robots for welding since 2013.

An example of application can be seen on https://www.youtube.com/watch?v=iJDLz8SOJIE.

16.2.4 Potential welding automation applications for bridge building

An obvious example for possible robotic welding of shorter welds in varying positions also with limited access could be the fillet welds between diaphragms/stiffeners, deck plates and troughs, see Figure 16-8.

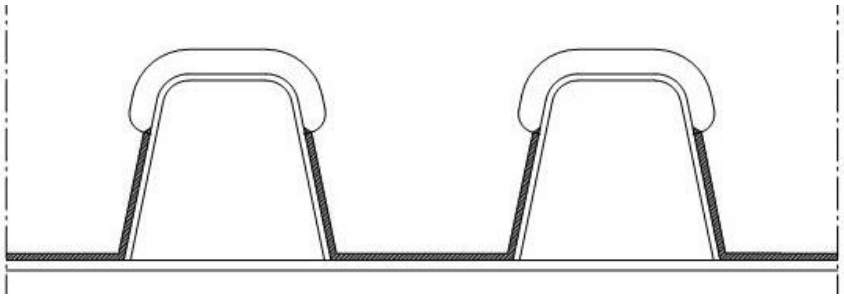

Figure 16-8 Fillet welds between diaphragms/stiffeners, troughs and deck are an obvious case for robotic welding

The recent advances within robotic welding have made it possible to place the robot in roughly correct position, and then let it locate the position of joints to be welded by itself. After some initial measurements by means of a laser sensor, the joints are tack welded and subsequently fully welded. The concept could be as shown in Figure 16-9.

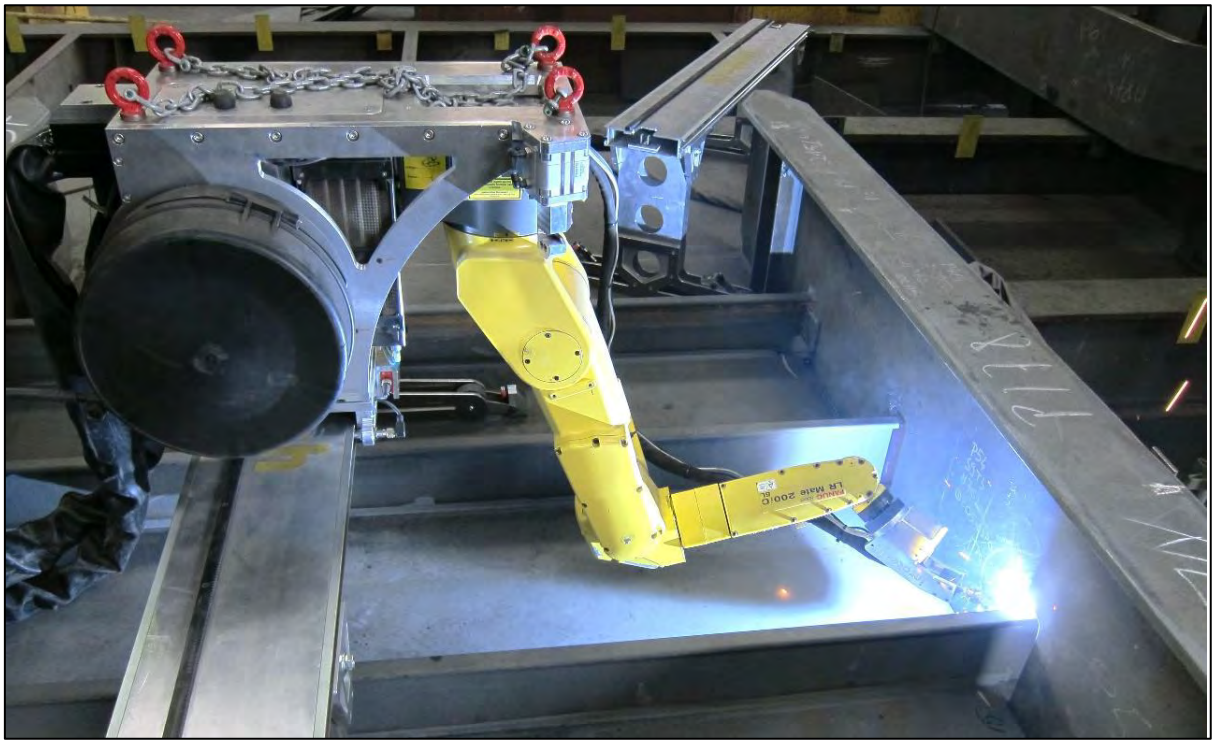

Figure 16-9 Robotic welding concept which might also be used for fillet welds between diaphragms/stiffeners, troughs and deck

Another application could be the welds between diaphragm trusses and flanges, see Figure 16-10.

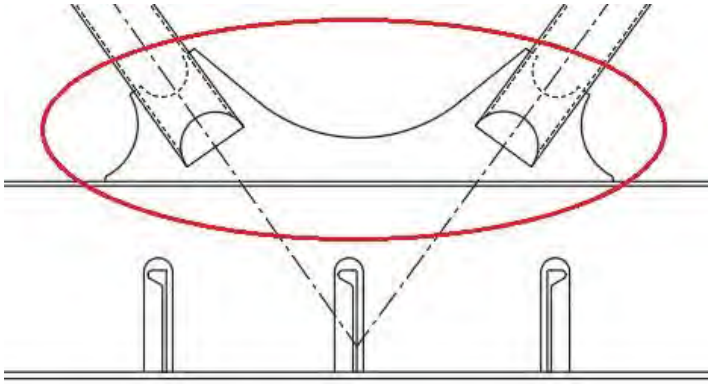

Figure 16-10 Joints between diaphragm trusses and flanges can be another case for robotic welding

Based on experience from shipyard applications, a duty cycle (amount of time the weld arc is actually on) of 60-70% can be expected. A suitable welding process would be flux cored arc welding. It is expected that one operator could control a couple of robots.

16.3 Construction of cable stayed bridge

The construction of the cable stayed bridge is described with the following stages:

- Temporary access roads and ground works
- Construction of the approach bridge
- Construction of abutment and piers
- Construction of the tower
- Construction of the bridge deck
- Construction of the cable stayed bridge deck
    - Erection of the pier table
    - Balanced cantilever construction
    - Closing the side span
    - Completion of the main span deck
- Installation of stay cables

The construction of the cable stayed bridge contains working processes that are well known and straight forward. The bridge is situated on shore except that a temporary bridge or embankment fill is required to provide access road to Svarvahelleholmen.

The works start with access roads and ground works for the south abutment, tower foundation and side span piers, with access roads between these sites. After preparation of the ground, the foundations can be casted. Jump formwork is then used for construction of the lower tower legs and piers. Temporary strutting between the tower legs is required due to their inclination.

After completion of piers, span-by-span construction of the concrete side spans can begin. An overhung or underhung moving scaffolding system can be used, and the scaffolding system is shifted along the bridge span by span, with in situ concrete works. The bridge deck is cast monolithically

without bearings to the pier tops. The bridge structure is longitudinally post-tensioned as necessary for the construction stage. Full tensioning can await completion of the concrete works.

The tower cross beam is cast in-situ supported by temporary scaffolding (truss) spanning between the legs. Hereafter the tower legs are cast by climbing formwork, alternatively by slip forming. Steel boxes for the stay anchorages are placed one by one while the concrete progress towards the top. Where the two legs join at level +175, the jump-form is shifted to a full-width form, used to the very top of the tower at +220.

Once constructed, the steel bridge "tower segment" is shifted in between the tower legs from the main span side. Then balanced erection of steel deck segments, 20 m long, is carried out. The water between the Svarvahelleholmen and Reksteren allows the side-span segments to be lifted off the barges also to this side, i.e. no steel element need to be transported on the ground.

When a steel segment has been lifted by the derrick crane and the joint is partly welded, the stays are installed. The cable is formed by individual strands that are pulled from the top and anchored at the bottom. When the stays are complete, and the steel segment joint is partly welded, the derrick crane can be moved further out ready for the next section. The segment installation continues until the segment towards the concrete spans is in place. The joint will be with in-situ stich concrete or grout, followed by tensioning of the longitudinal cables and bolts going through the joint.

The cycle of erecting steel segments is estimated to be in the range of 10-14 calendar days. It can however be done in parallel both sides for the first 2*7 segments.

The above erection schedule implies that the cable stayed bridge shall stay the winter fully erected without connected to the floating bridge. This situation is analysed and found not being critical.

The bridge finishing works, pavement, barriers, bearings etc. are finally installed.

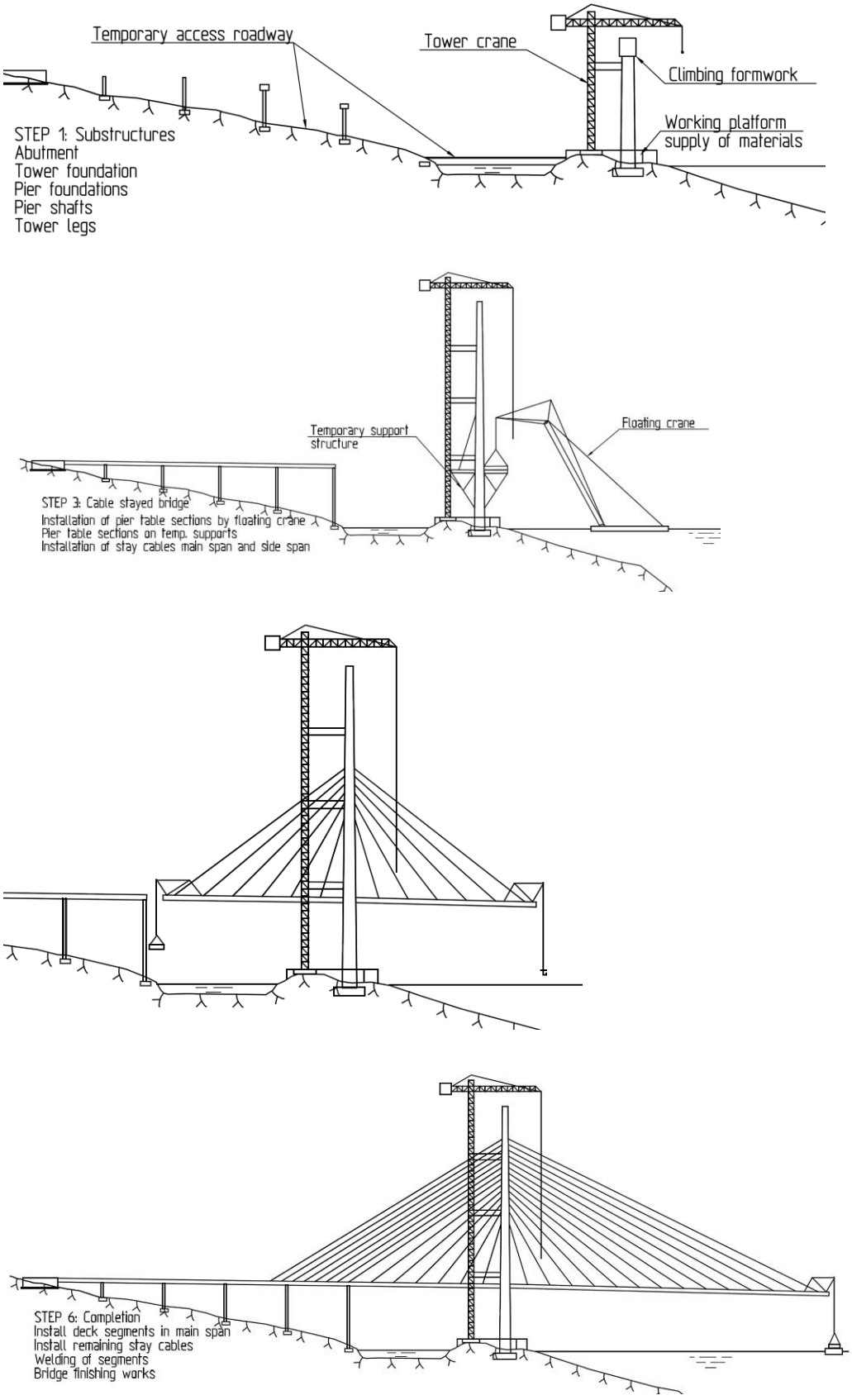

Figure 16-11 Construction of cable stayed bridge

16.4 Construction of north abutment

The north abutment is a reinforced concrete structure, which can be constructed in situ using traditional formwork after an access to main land is established. The concrete structure is filled with iron ore. A steel transition structure is lifted by a floating crane and connected to the abutment by pre-stressing cables as part of the abutment construction. The south end of this structure interfaces the “standard” bridge girder of the floating bridge.

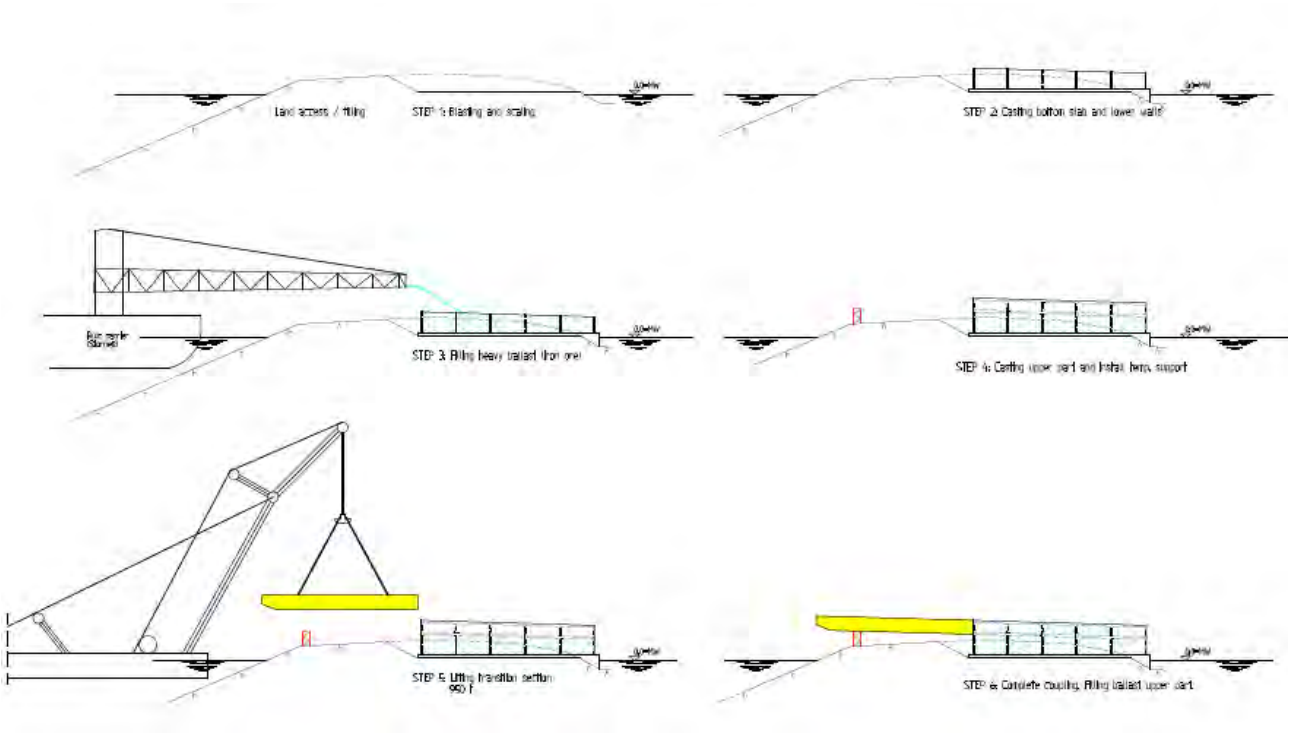

Figure 16-12 Construction of north abutment

16.5 Mooring system pre-installation

The bridge concept has 12 mooring lines.

It is assumed that a mobilisation base close to the bridge location may be used for installation of the anchors and mooring lines, e.g. Eldøyane at Stord.

The anchors are proposed installed without the mooring line attached about one year before the bridge installation to ensure settling of the seabed before the anchors are loaded. All the anchors are suctions anchors and will be installed by a crane vessel with WROVs.

The mooring lines are installed in a separate installation campaign planned such that all mooring lines are installed in due time before assembly of the floating bridge at bridge location starts and are planned to be temporarily wet stored at seabed.

16.6 Assembly of bridge sections

The floating bridge assembly will be performed on barges in a sheltered fjord. The high floating bridge and low floating bridge are planned to be assembled in Søreidsvika with slightly different methods.

For the low floating bridge 125 m sections will be constructed on a barge. The pontoon and column will be floated in and welded to the bridge section. The bridge section will be skidded 125 m and the

process is repeated until the low floating bridge is completed. The process is shown in the figures below.

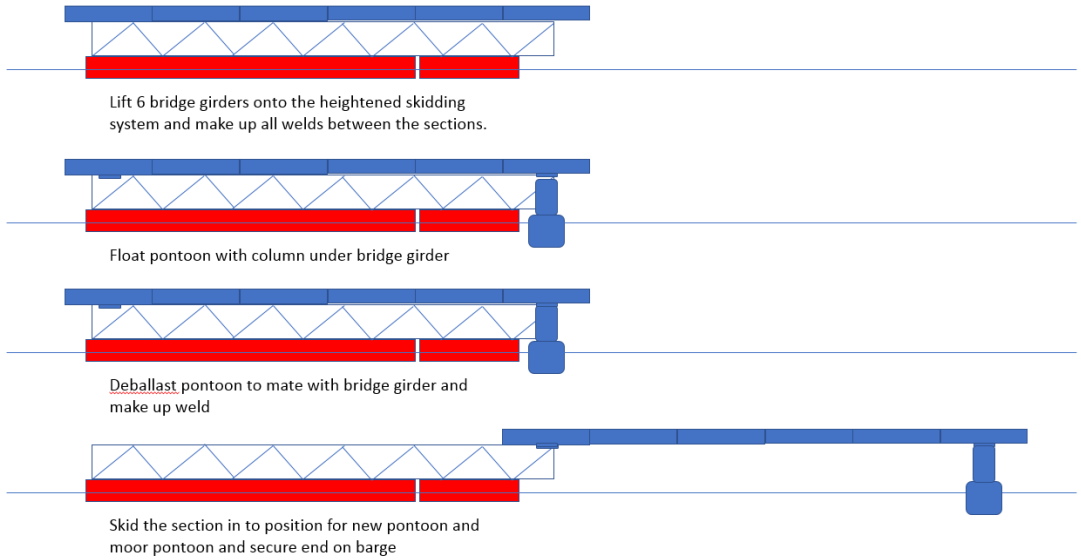

Figure 16-13 Low floating assembly sequence – 1

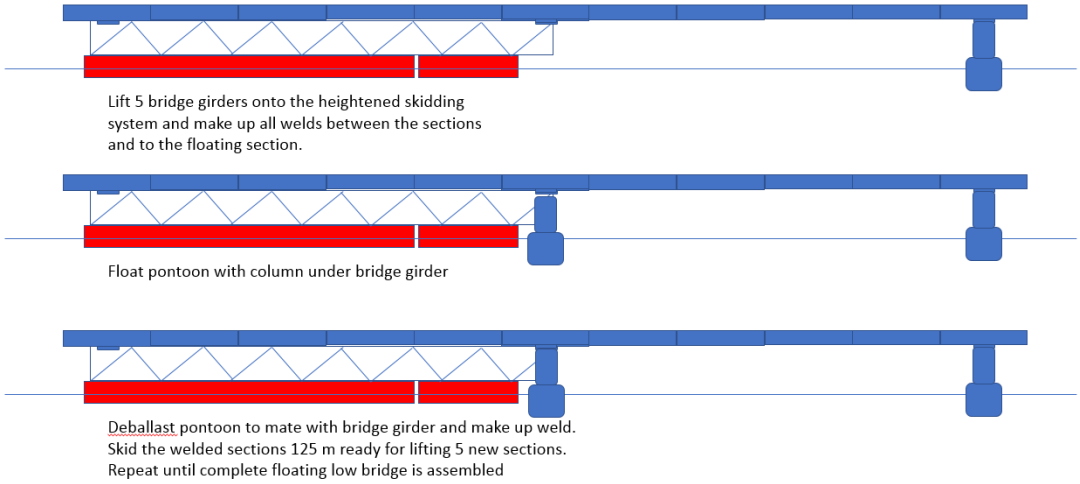

Figure 16-14 Low floating assembly sequence – 2

The assembly method for the high floating bridge is presented in the illustrations below:

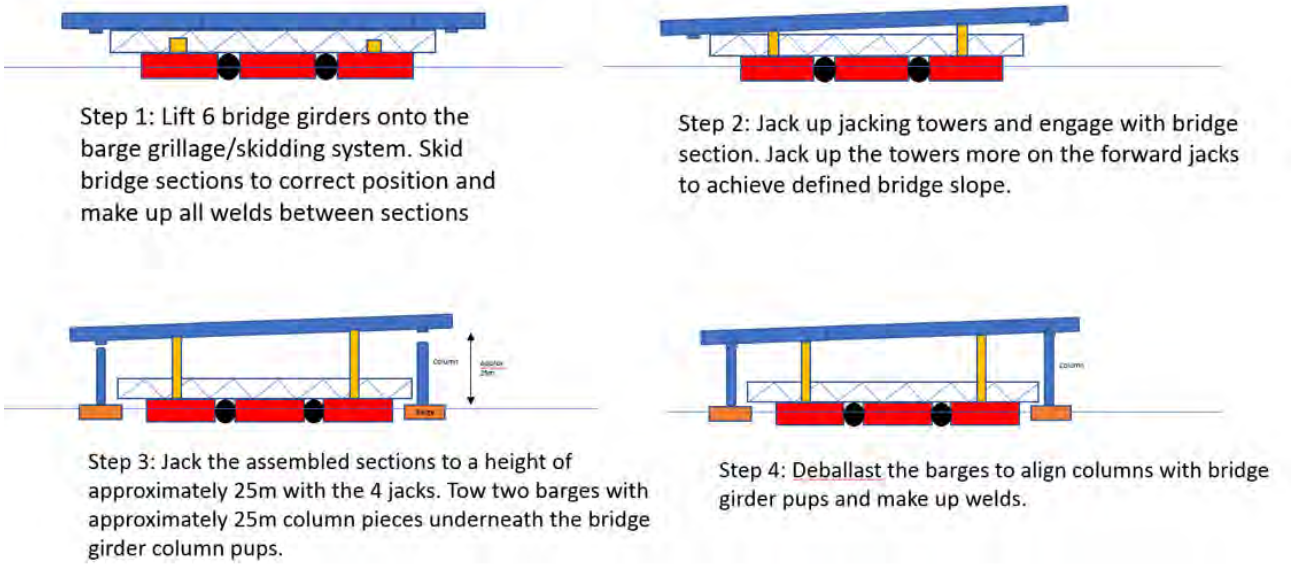

Figure 16-15 High floating assembly sequence – 1

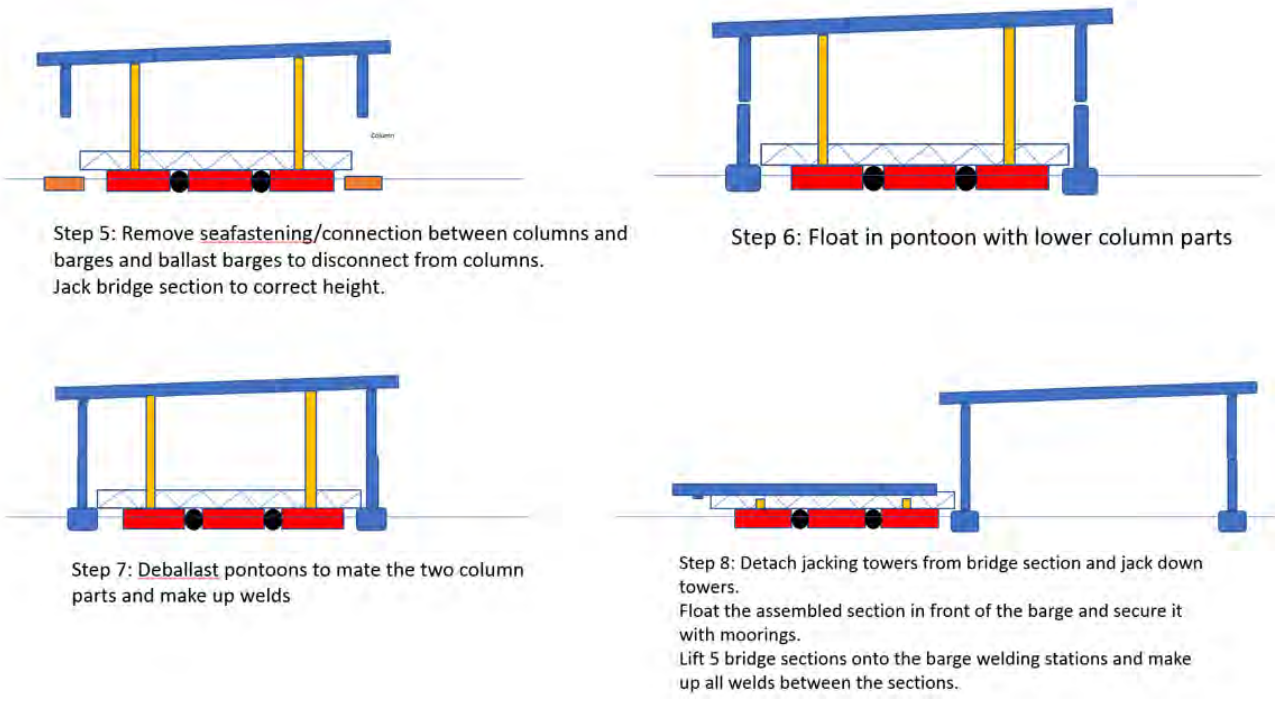

Figure 16-16 High floating assembly sequence – 2

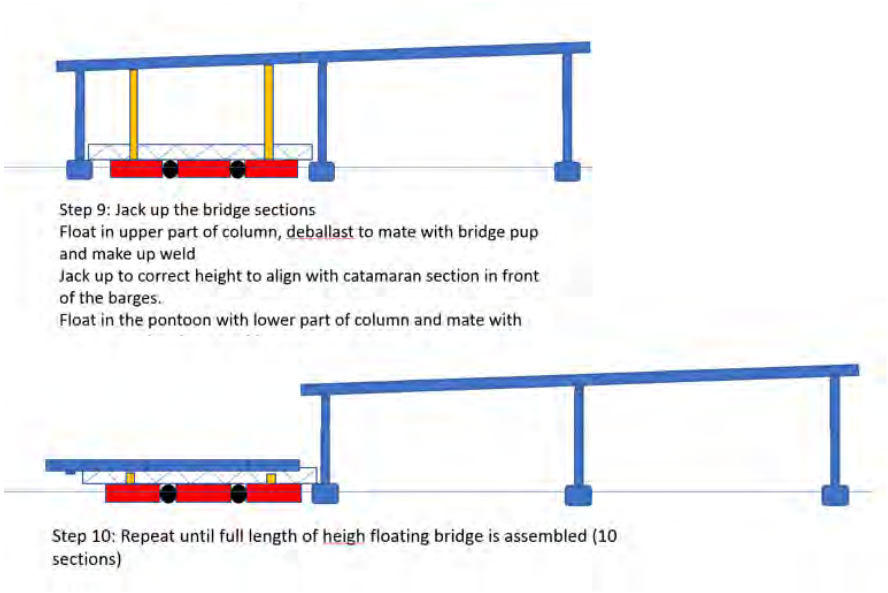

Figure 16-17 High floating assembly sequence – 3

16.7 Towing of bridge sections

A typical illustration of the towing operation is given below with Orcaflex screenshot showing the towing from the fabrication site in Søreidsvika.

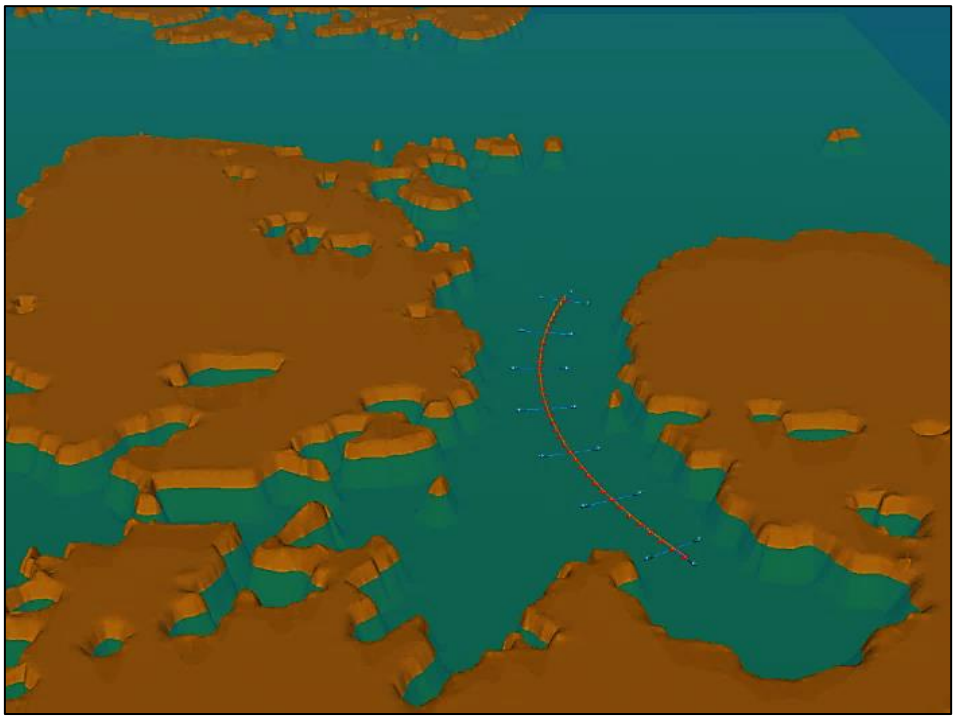

Figure 16-18 Connect rest of towing fleet and commence tow out from fjord

A total of 12 off 200 tonnes bollard pull tugs is needed for the towing operation. This is based on the following considerations:

- Weather vaning is included for by assuming the vessel is aligned with the longitudinal axis towards the weather. In this situation, it is possible to utilize vessels connected on both sides of the bridge. It is further assumed that each tug on average can provide pull at 45 degrees relative to the weather.

- An average bollard pull of 200 tonnes is considered for each vessel, with an efficiency factor of 0.8.
- In total each vessel is on average capable of providing 113 tonnes force towards the weather.
- It is considered that an even number of towing vessels is applied to achieve a symmetric setup.

The bridge integrity has been verified for a towing force of 600 tonnes onto one pontoon.

The towage will be managed with a tug management system. The system will be based on a standard system for towing of rigid structures (vessels, platforms) but will be adjusted such that it will also incorporate the deformation monitoring of the bridge. A secondary tow management system will also need to be included.

All installation operations are planned as weather restricted operations. The towing operations are planned to have a location in Bjørnafjorden, where the tow can survive a seasonal storm

16.8 Installation of floating bridge

First, a smaller north section will be towed to site and connected to the north abutment transition section as shown below. The floating section will be ballasted up and down to account for the tidal variations during the installation.

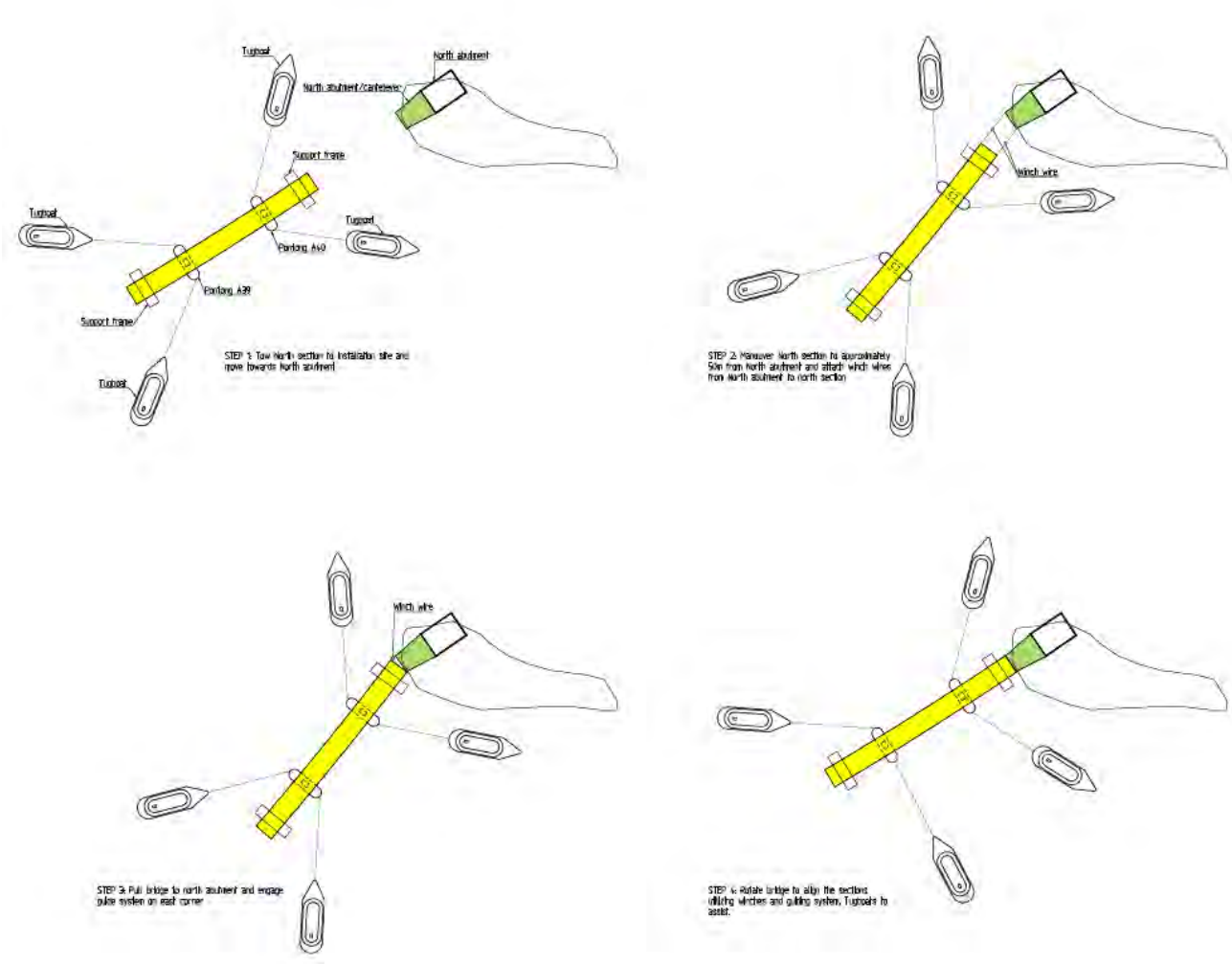

The floating bridge section will be towed to site and connected first to the north section and then to the cable stayed bridge as shown below:

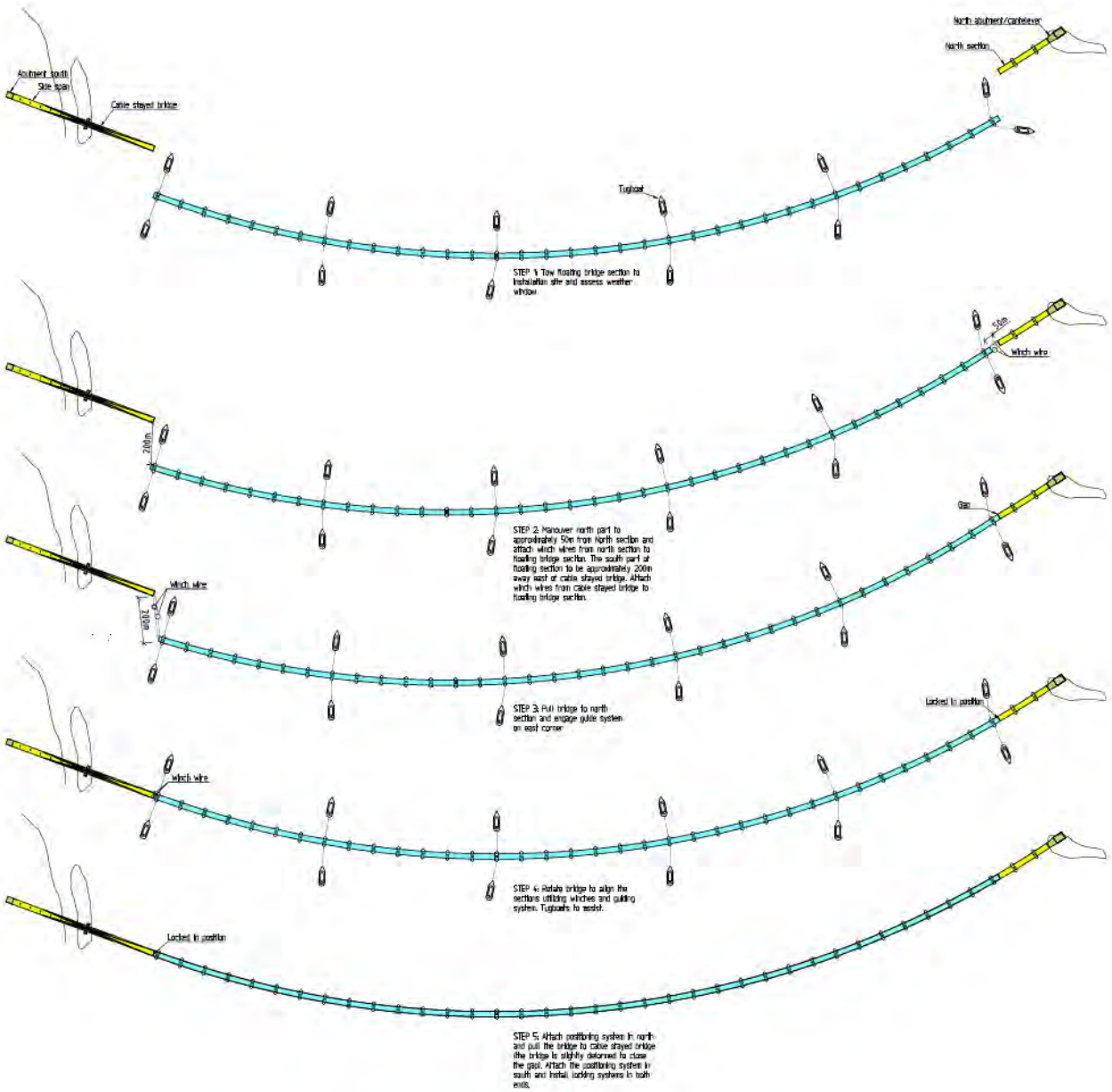

Figure 16-19 Installation sequence of K12 floating bridge

The guiding and connection of the floating sections will be performed with 3 different systems and are based on the same principles for all three connections. The guiding system will create the initial contact point between two bridge sections. Once the guiding system is engaged, one can connect the “positioning system”. The positioning system enables alignment of the sections in all directions and secures the bridge until the “locking system” to be installed. The locking system secures the bridge and minimize the strain during welding. It will be able to withstand a summer-storm. Illustrations are shown below:

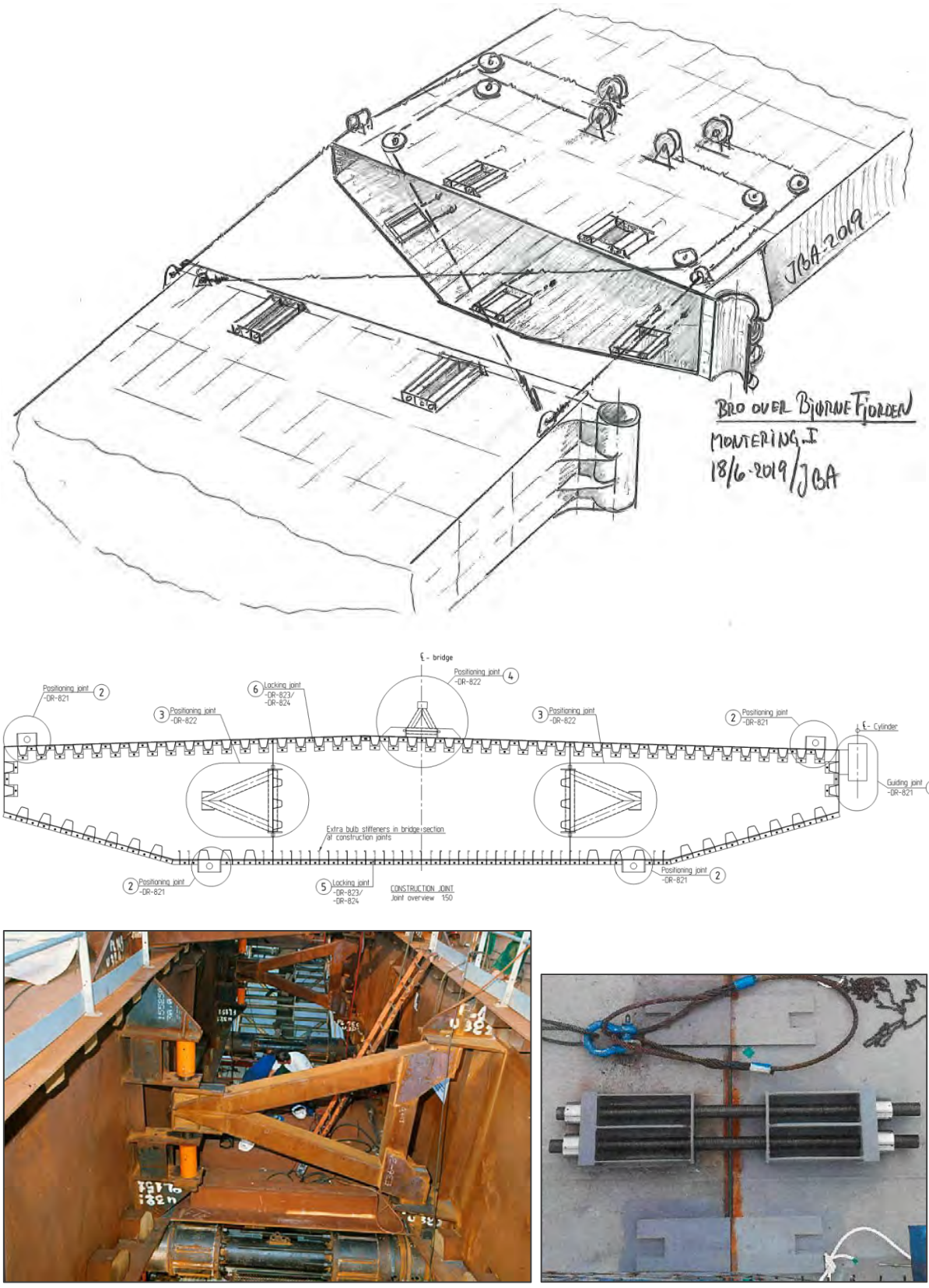

Figure 16-20 Guiding system, positioning system and locking system illustrations and pictures

16.9 Mooring lines hook-up

After the connection of the floating bridge in both ends, the mooring lines will be hooked up to the pontoons from wet storage and tensioned up.

The installation vessel picks up the mooring line from the seafloor and pulls the mooring line through the chain stopper on the pontoon and pre-tensions the mooring line to the defined pre-tension.

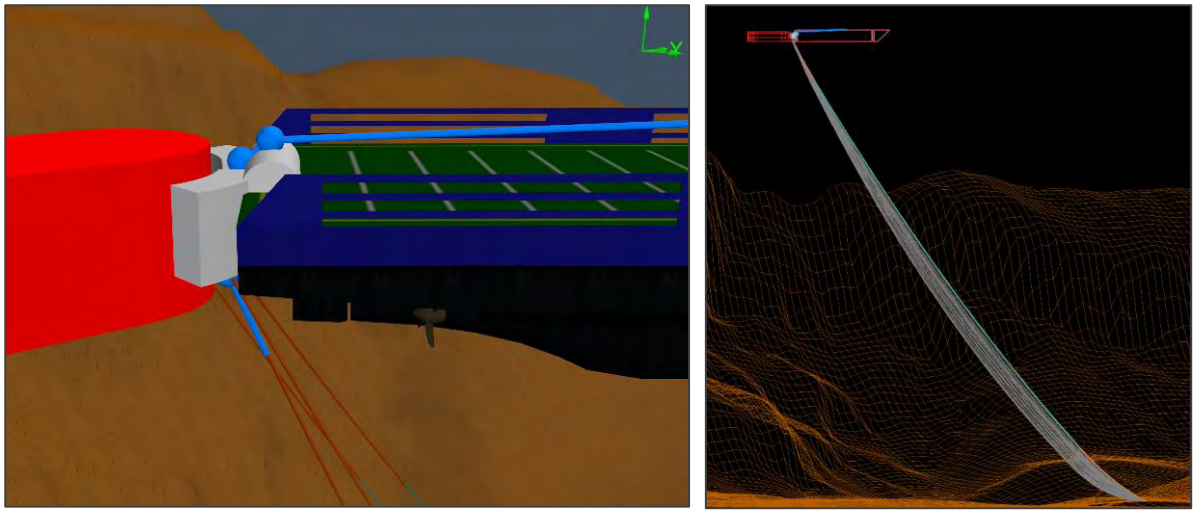

Figure 16-21 Mooring line tensioning at pontoon with bumper. Only very low thrust forces are needed in this configuration.

16.10 Final on-site welding

After all mooring lines are connected, welding in the north and south segments can commence. The locking system is designed such that strains in the weld are kept to a minimum.

17 Material technology and steel in marine environment

17.1 General evaluations

The bridge design life is 100 years and this document discusses material selection and means of providing corrosion protection to limit the need for future inspections, maintenance, and replacements. The recommended solutions are summarised in the table below.

The most severe exposure conditions are in the splash zone and in this area carbon steel will be replaced by a corrosion resistant alloy, 25Cr DSS. Welding of carbon steel to 25Cr DSS is fully manageable provided properly qualified procedures and suitable materials are used.

High level cathodic protection (CP) calculations have been performed. The anode weight requirements vary dependent on the selected CP design life and extent of coating on the 25Cr DSS plates. Detailed calculations should be performed in next phase.

Corrosion allowances (CA) for the mooring chains have been evaluated based on standards and requirements included in the SVV design basis. Since the top chain is situated below the splash zone, the same CA as for the bottom chain is proposed (0.2 mm/year).

The recommended solutions are summarized below:

Table 17-1 Recommended solutions

Bridge section	Generic material selection	Proposed corrosion protection
Upper section: Underside of road structure, columns and pontoon above splash zone	Carbon steel	SVV system 2
Pontoon, splash zone and submerged section	Carbon steel with solid 25 Cr duplex stainless steel in splash zone	NORSOK System 7B + aluminium based sacrificial anodes
Ballast water tank, active tank	Carbon steel	NORSOK system 7B + zinc based sacrificial anodes
Ballast water tank, passive tank	Carbon steel	NORSOK system 1
Empty sections / voids in the pontoon with active dehumidification	Carbon steel	NORSOK system 3G
Empty sections / voids in the pontoon *without* active dehumidification	Carbon steel	NORSOK system 1

For further details, see appendix O.

18 References

[1] AMC, “SBJ-33-C5-AMC-90-RE-107 : Appendix G: Global Analyses - Response Rev. 0,” 15-08-2019.

[2] AMC, “SBJ-33-C5-AMC-22-RE-112 : Appendix L: Design of Cable Stayed Bridge and Abutments Rev. 0,” 15-08-2019.

[3] AMC, “SBJ-33-C5-AMC-26-RE-113 : Appendix M: Anchor systems Rev. 0,” 15-08-2019.

[4] AMC, “SBJ-33-C5-AMC-90-RE-106 : Appendix F: Global Analyses - Modelling and assumptions Rev. 0,” 15-08-2019.

[5] AMC, “SBJ-33-C5-AMC-22-RE-111 : Appendix K: Design of Floating Bridge Part Rev. 0,” 15-08-2019.

[6] AMC, “SBJ-33-C5-AMC-20-RE-105 : Appendix E: Aerodynamics Rev. 0,” 15-08-2019.

[7] AMC, “10205546-11-NOT-088 :AMC status 2 - Variable static loads,” 29.03.2019.

[8] AMC, “10205546-11-NOT-059 AMC status 2 - Estimation of extreme response using the AUR method. Rev. 0,” 29.03.2019.

[9] Statens Vegvesen, “SBJ-32-C4-SVV-90-BA-001 Design basis. Rev. 0,” 19.11.2018.

[10] Statens Vegvesen, “Vehicle properties for comfort evaluation,” 04.02.2019.

[11] AMC, “SBJ-33-C5-AMC-21-RE-108 : Appendix H: Global Analyses - Special studies Rev. 0,” 15-08-2019.

[12] I. Kovacic, R. Rand and S. M. Sah, “Mathieu's Equation and Its Generalizations: Overview of Stability Charts and Their Features,” *Applied Mechanics Reviews,* 2018.

[13] J. L. Humar, Dynamics of structures, CRC Press, 2012.

[14] O. Øiseth, B. Costa and A. Fenerci, “SBJ-32-C4-NTNU-22-RE-001 "Dynamic stability of elastic nonlinear systems subjected to random excitation",” Statens vegvesen, 2018.

[15] C. Dørum, “304624-1-A-0028, Skipsstøt, varsel om endringer i design basis,” SVV eRoom, 04.02.2019.

[16] AMC, “"10205546-11-NOT-196 : Uncertainty assessment, Rev. 0,” 15.08.2019.

[17] AMC, “10205546-11-NOT-193 Long-term wave response, rev. 0,” 15.08.2019.

[18] F.-I. G. Giske, “Long-Term Extreme Response Analysis of Marine Structures Using Inverse Reliability Methods,” Norwegian University of Science and Technology (NTNU), Trondheim, 2017.

[19] F.-I. G. Giske, K.-A. Kvåle, B. J. Leira and O. Øiseth, “Long-term extreme response analysis of a long-span pontoon bridge,” *Marine Structures,* vol. 58, pp. 154-171, 2018.

[20] E. Vanem, “A comparison study on the estimation of extreme structural response from different environmental contour methods,” *Marine Structures,* vol. 56, pp. 137-162, 2017.

[21] W. Chai and B. J. Leira, “Environmental contours based on inverse SORM,” *Marine Structures,* vol. 60, pp. 34-51, 2018.

[22] E. Ross, O. C. Astrup, E. Bitner-Gregersen, N. Bunn, G. Feld, B. Gouldby, A. Huseby, Y. Liu, D. Randell, E. Vanem and P. Jonathan, “On environmental contours for marine and coastal design,” in *Proceedings of the ASME 2019 38th International Conference on Ocean, Offshore and Arctic Engineering (OMAE 2019)*, Glasgow, 2019.

[23] G. Feld, P. Jonathan and D. Randell, “On the estimation and application of directional design criteria,” in *Proceedings of the ASME 2019 38th International Conference on Ocean, Offshore and Arctic Engineering (OMAE 2019)*, Glasgow, 2019.

[24] AMC, “10205546-12-NOT-065 Moorling line damping, rev. 0,” 18.02.2019.

[25] AMC, “10205546-11-NOT-095 Rev1. Analytical mooring line damping,” 2019.

[26] AMC, “SBJ-33-C5-AMC-90-RE-121 : Appendix U: Verification Rev. 0,” 15-08-2019.

[27] Statens Vegvesen, “SBJ-32-C4-SVV-90-BA-001 Design basis. Rev 0.,” 19.11.2018.

[28] AMC, “10205546-11-NOT-076 AMC status 2 - Plastic capacity of column,” 29.03.2019.

[29] W.-C. Xie, Dynamic stability of structures, Cambridge University Press, 2006.

[30] Rambøll, “1100025487-1793395602-98 BJØRNAFJORDEN SKIBSSTØDSANALYSE FOR SIDEFORANKRET FLYDEBRO – BEGRÆNSET HASTIGHED, Rev 0,” 2018.

[31] AMC, “SBJ-33-C5-AMC-27-RE-110 : Appendix J: Ship collision Rev. 0,” 15-08-2019.

[32] AMC, “SBJ-33-C5-AMC-22-RE-109 : Appendix I: Fatigue analyses Rev. 0,” 15-08-2019.

[33] AMC, “10205546-01-NOT-055 Programvare,” 14.02.2019.

[34] DNV GL Software, “Sesam User Manual, WASIM v. 5.5,” 2017.
[35] DNV GL Software, “Sesam User Manual, WADAM v. 9.4,” 2017.
[36] AMC, “10205546-11-NOT-059 Estimation of extreme response using the AUR method, rev. 0,” 29.03.2019.
[37] AMC, “"10205546-13-NOT-194 Shear lag and buckling effects of bridge girder concept 12",” 15.08.2019.